Proceedings of:
ASME TURBO EXPO 2003
June 16-19, 2003, Atlanta, GA

GT-2003-38580

Measurements and Predictions of Surface Roughness Effects on Turbine Vane Aerodynamics

R. J. Boyle
NASA Glenn Research Center
Cleveland, Ohio
Robert.J.Boyle@grc.nasa.gov

R. G. Senyitko
QSS Group, Inc.
Cleveland, Ohio
Richard.G.Senyitko@grc.nasa.gov

ABSTRACT

The aerodynamic performance of a turbine vane was measured in a linear cascade. These measurements were conducted for exit-true chord Reynolds numbers between 150,000 and 1,800,000. The vane surface rms roughness-to-true chord ratio was approximately 2×10^{-4}. Measurements were made for exit Mach numbers between 0.3 and 0.9 to achieve different loading distributions. Measurements were made at three different inlet turbulence levels. High and intermediate turbulence levels were generated using two different blown grids. The turbulence was low when no grid was present. The wide range of Reynolds numbers was chosen so that, at the lower Reynolds numbers the rough surfaces would be hydraulically smooth. The primary purpose of the tests was to provide data to verify CFD predictions of surface roughness effects on aerodynamic performance. Data comparisons are made using a two-dimensional Navier-Stokes analysis. Both two-equation and algebraic roughness turbulence models were used. A model is proposed to account for the increase in loss due to roughness as the Reynolds number increases.

Nomenclature

C_p	-	Pressure coefficient, $(P_{t-1} - P)/(P_{t-1} - P_2)$
C	-	True chord
h	-	Roughness height
k	-	Turbulent kinetic energy
l	-	Length scale
M	-	Mach number
Re	-	Reynolds number
s	-	Surface distance
Tu	-	Turbulence intensity
U	-	Velocity
Y	-	Loss coefficient, $(P_{t-1} - P_{t-2})/(P_{t-1} - P_2)$
μ	-	Molecular viscosity
ρ	-	Density
θ	-	Momentum thickness
ω	-	Specific dissipation rate

Subscripts

A	-	Area averaged
FS	-	Freestream
IN	-	Gas inlet
t	-	Total
1	-	Vane row inlet
2	-	Vane row exit

INTRODUCTION

Surface roughness can adversely affect turbomachinery blade row efficiencies. Studies by Kind et al.(1); Boynton et al.(2); and by Bammert and Standstede(3,4) reported turbine efficiency decreases of up to several points as a result of surface roughness. On the other hand, Harbecke et al.(5) found that profile loss for a turbine rotor was not increased until the roughness exceeded a critical value. Stabe and Liebert(6) found that there was a four point(0.04) reduction in stator kinetic loss coefficient when the ceramic coating of a stator vane was lightly polished.

Surface roughness can be the result of deposition, erosion, or the blade surface finish. Both deposition and erosion can alter the throat area so as to affect the passage flow rate. Bons et al.(7) and Taylor(8) discuss the roughness characteristics of many blades from various manufacturers. Bons et al.(7) grouped the blades by the causes for the surface roughness, and large variations in roughness height were seen. El-Batsh and Haselbacher(9) predicted a three point increase in the total pressure loss coefficient of a vane due to ash particle deposition after only 36 hours of service. Ceramic vanes have surface roughness typically greater than that of metal vanes. The benefits of the higher temperature capability of ceramic blades could be outweighed by the increase in losses resulting from surface roughness.

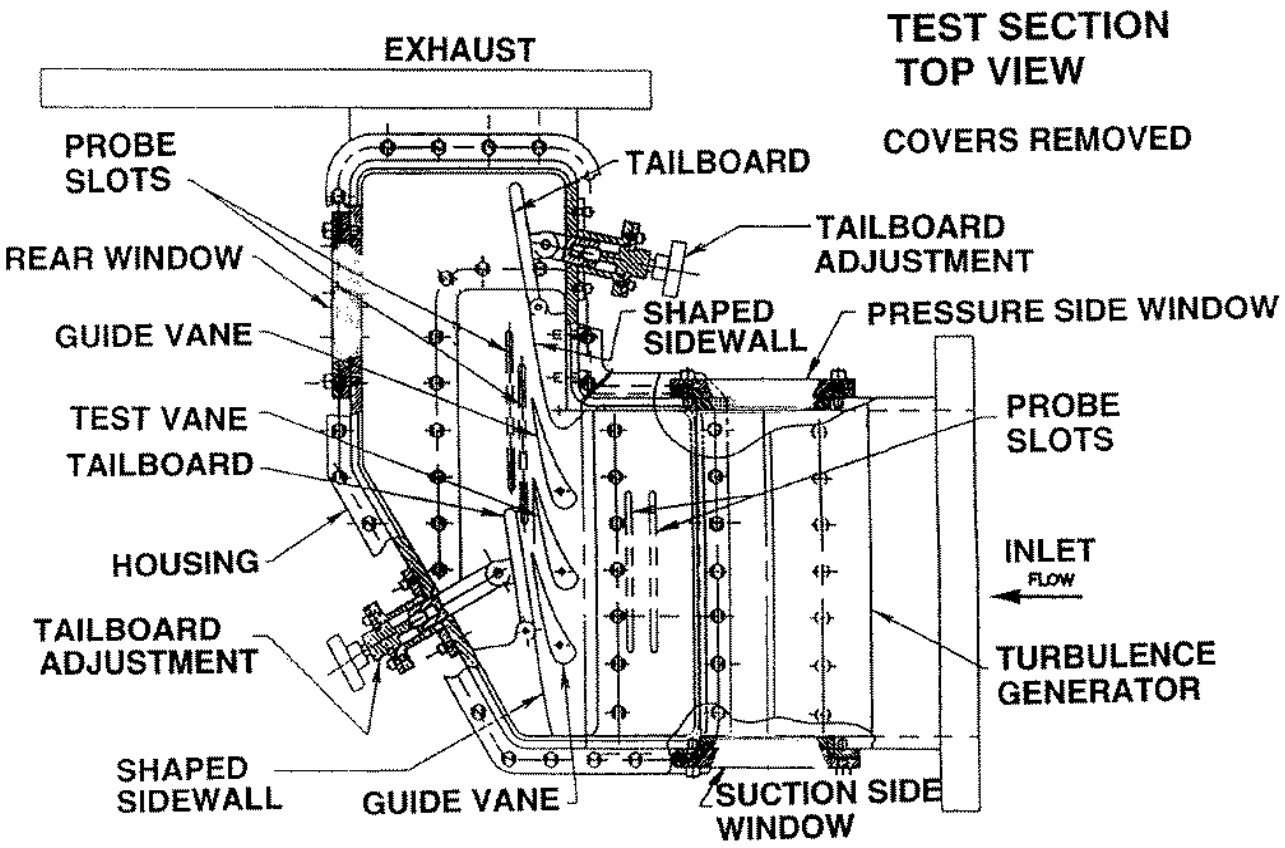

Fig. 1 Overall view of test section.

A surface of given roughness could be hydraulically smooth at low Reynolds numbers, but at higher Reynolds numbers roughness could significantly affect loss. El-Batsh and Haselbacher(9) showed that deposition can affect the passage flow path, and increase losses by increasing surface diffusion or trailing edge thickness. This is a potential flow effect, and is not directly related to surface roughness. To isolate surface roughness effects, smooth and rough blade flow paths should be the same.

Prediction for the effects of surface roughness have been reported by several authors. Taylor et al.(10) described an analysis that accounted for the geometry of the roughness elements. Cebeci and Chang(11) accounted for roughness by modifying the mixing length in an algebraic turbulence model. Wilcox(12) proposed a two equation $k-\omega$ turbulence model which accounted for surface roughness in the boundary condition on ω.

The work presented herein compares total pressure loss for smooth and rough vanes over a range of Reynolds and Mach numbers for three turbulence levels. Predictions using algebraic and two-equation turbulence models are compared with data to determine an appropriate model to predict the effects of roughness on aerodynamic performance. The smooth and rough vane profiles were closely matched, so that the differences between the flow fields were negligible. The vane shape was suitable for ceramic engine applications. Smooth vane data were previously reported in reference 13. The work herein concentrates on loss differences between the rough and smooth vanes, and on approaches to predicting surface roughness effects.

Description of Facility

Vane aerodynamic measurements were conducted in a high aspect ratio linear cascade. The overall view of the cascade is shown in figure 1. Table I shows the range of inlet total pressures and exit true chord Reynolds numbers for which data were obtained at each of four isentropic exit Mach numbers. Table II gives characteristics of the vane. There are three vanes and two shaped sidewalls with adjustable tailboards. Vane pressure measurements on the three vanes were used to determine periodicity. Thermocouple and Pitot probes upstream of the vane gave the vane inlet conditions. The high aspect ratio was chosen to achieve two-dimensional flow in the midspan region. Results are compared with two-dimensional CFD analyses. Reynolds and Mach numbers can be varied independently.

Inlet survey slots 4.3 and 8.2cm upstream of the vane, and exit survey slots 1.27 and 2.54cm downstream of the vane are shown in figure 1. These slots extended approximately two vane pitches. Further details regarding the test facility, and the approaches taken for the measurements, are given in references 13 and 14. Reference 13 also discusses issues that arose regarding turbulence measurements in the facility.

Table I. Operating range of Test conditions

M_2	P_{t-1} (atm)	Re_c $\times 10^{-6}$
0.3	0.20	0.133
	1.4	0.934
0.5	0.20	0.207
	1.4	1.450
0.7	0.27	0.350
	1.2	1.570
0.9	0.30	0.440
	1.2	1.760

Table II. Vane Characteristics

Axial Chord, C	5.18 cm
True Chord	10.40 cm
Pitch	8.26 cm
Span	21.59 cm
Trailing edge thickness	0.26 cm
Flow turning angle	75°

Data were obtained at low, medium, and high turbulence intensities. The turbulence intensity was approximately 1% when no turbulence grids were used. Medium and high turbulence was achieved using different blown grids as described in reference 13. These grids were 24.7 cm upstream of the vane leading edges, and differed in the size and number of tubes oriented in the spanwise direction. With blown air turbulence intensity was spatially uniform. The smaller diameter tubes produced an inlet turbulence of approximately 8%, and the larger tubes produced a level of approximately 17%. Without air, the small tubes gave a spatially varying turbulence intensity of between 3 and 6%. Results for the large tube and small tube grids are referred to as large grid and small grid results respectively.

As discussed by Price et al.(15), ceramic vanes have relatively thick trailing edges. The vane tested is shown in figure 2. This vane shape was originally tested by Schwab(16), and was used for the smooth vane tests of reference 13. It was chosen for this work because it is appropriate for a ceramic vane applications. Coordinates are given in the references. The rough vane was formed by spraying a ZrO coating on a vane that was 0.3mm undercut from the shape of the smooth vane. Templates attached to the test vane ends insured that rough and smooth vanes had the same profiles.

Roughness measurements. Roughness traces were obtained for the vane using a Talysurf profilometer. A summary of the results are presented in Table III for both the rough and smooth vanes. The average absolute difference from the mean, h_a is somewhat less than the average rms value, h_{RMS}. The smooth vane has a roughness that is less than ten percent of that of the rough vane. Roughness effects for the smooth vane are expected to be seen at a Reynolds number approximately an order of magnitude greater than the Reynolds number at which the rough vane shows roughness effects. The average h_a value of $14\mu m$ is

Table III. Vane roughness characteristics.

Trace	h_{RMS} mm	h_a mm	Skewness	Kurtosis
Rough vane				
1	0.0177	0.0140	0.206	-0.195
2	.0205	.0159	-0.441	0.232
3	.0175	.0139	-0,010	-0.036
4	.0170	.0130	-0.085	0.449
Avg.	0.0182	0.0142		
Smooth vane				
1	0.0014	0.0011	-0.984	2.107
2	.0015	.0011	-1.322	2.884
3	.0019	.0014	-1.319	2.657
4	.0018	.0013	-1.296	2.775
Avg.	0.0016	0.0012		

Fig. 2, Test vane and passage.

near the high end of the roughness range for the in service blades measured by both Bons et al.(7) and Taylor(8). Kurtosis was calculated using the same definition as Taylor(8). The values of Skewness and Kurtosis are with the range of values given by Bons et al.(7) and Taylor(8).

The equivalent roughness height, h_{EQ}, is the significant roughness parameter used in the analysis. The importance of the equivalent height to losses is discussed by Abuaf et al.(17). Table IV gives the equivalent roughness height using different correlations. The variation in equivalent roughness height among different correlations for the same h_{RMS} was much greater than the variation in h_{RMS} Several authors have proposed approaches to determine the equivalent sand grain roughness to be used in analytic models. To obtain the equivalent roughness height, the roughness trace is used to determine the characteristics of an assumed roughness shape. The roughness trace was taken as the projection of either cones or hemispheres. Calculations are shown for two different assumptions regarding what constitutes a peak in the roughness profile. For one assumption, a peak was counted only if the average value was exceeded. In the other assumption, it exceeded the average value by more than the rms height. This assumption resulted in taller peaks spaced further apart.

Table IV. Equivalent height ratio

	Equivalent Height Roughness Model							
Trace	h_{RMS} mm	Sigal & Danberg-2D	Sigal & Danberg-3D	Dvorak	Dirling	Waigh & Kind	van Rij et al.	Bons
		$h_{\mathrm{PEAK}} > h_{\mathrm{AVG}}$ - Cone Model						
		$h_{\mathrm{EQ}}/h_{\mathrm{RMS}}$	$h_{\mathrm{EQ}}/h_{\mathrm{RMS}}$	$h_{\mathrm{EQ}}/h_{\mathrm{RMS}}$	$h_{\mathrm{EQ}}/h_{\mathrm{RMS}}$	$h_{\mathrm{EQ}}/h_{\mathrm{RMS}}$	$h_{\mathrm{EQ}}/h_{\mathrm{RMS}}$	$h_{\mathrm{EQ}}/h_{\mathrm{RMS}}$
1	0.0177	2.041	0.453	0.729	0.772	1.502	0.428	21.4
2	0.0205	1.056	0.220	0.358	0.383	0.796	0.199	20.6
3	0.0175	1.366	0.284	0.494	0.528	0.979	0.259	22.2
4	0.0170	1.789	0.414	0.632	0.633	1.363	0.394	30.7
Avg.	0.0182	1.563	0.343	0.562	0.579	1.160	0.309	23.7
		$h_{\mathrm{PEAK}} > h_{\mathrm{AVG}}$ - Hemisphere model						
		$h_{\mathrm{EQ}}/h_{\mathrm{RMS}}$	$h_{\mathrm{EQ}}/h_{\mathrm{RMS}}$	$h_{\mathrm{EQ}}/h_{\mathrm{RMS}}$	$h_{\mathrm{EQ}}/h_{\mathrm{RMS}}$	$h_{\mathrm{EQ}}/h_{\mathrm{RMS}}$	$h_{\mathrm{EQ}}/h_{\mathrm{RMS}}$	$h_{\mathrm{EQ}}/h_{\mathrm{RMS}}$
1	0.0177	1.669	0.348	0.680	0.610	0.394	0.316	21.4
2	0.0205	0.798	0.152	0.313	0.295	0.444	0.132	20.6
3	0.0175	1.183	0.236	0.472	0.435	0.660	0.209	22.2
4	0.0170	1.337	0.283	0.549	0.487	0.750	0.258	30.7
Avg.	0.0182	1.247	0.255	0.504	0.457	0.562	0.229	23.7
		$h_{\mathrm{PEAK}} > h_{\mathrm{AVG}} + h_{\mathrm{RMS}}$ - Cone Model						
		$h_{\mathrm{EQ}}/h_{\mathrm{RMS}}$	$h_{\mathrm{EQ}}/h_{\mathrm{RMS}}$	$h_{\mathrm{EQ}}/h_{\mathrm{RMS}}$	$h_{\mathrm{EQ}}/h_{\mathrm{RMS}}$	$h_{\mathrm{EQ}}/h_{\mathrm{RMS}}$	$h_{\mathrm{EQ}}/h_{\mathrm{RMS}}$	$h_{\mathrm{EQ}}/h_{\mathrm{RMS}}$
1	0.0177	1.027	0.148	0.302	0.411	0.730	0.112	1.62
2	0.0205	1.167	0.176	0.341	0.447	0.859	0.138	1.64
3	0.0175	1.619	0.247	0.498	0.659	1.135	0.193	1.91
4	0.0170	2.275	0.419	0.727	0.837	1.702	0.358	4.74
Avg.	0.0182	1.522	0.248	0.467	0.671	1.109	0.200	2.48
		$h_{\mathrm{PEAK}} > h_{\mathrm{AVG}} + h_{\mathrm{RMS}}$ - Cone Model						
		$h_{\mathrm{EQ}}/h_{\mathrm{RMS}}$	$h_{\mathrm{EQ}}/h_{\mathrm{RMS}}$	$h_{\mathrm{EQ}}/h_{\mathrm{RMS}}$	$h_{\mathrm{EQ}}/h_{\mathrm{RMS}}$	$h_{\mathrm{EQ}}/h_{\mathrm{RMS}}$	$h_{\mathrm{EQ}}/h_{\mathrm{RMS}}$	$h_{\mathrm{EQ}}/h_{\mathrm{RMS}}$
1	0.0177	0.839	0.112	0.280	0.327	0.453	0.084	1.62
2	0.0205	0.883	0.122	0.298	0.344	0.479	0.092	1.64
3	0.0175	1.404	0.204	0.487	0.544	0.766	0.158	1.91
4	0.0170	1.702	0.286	0.631	0.642	0.936	0.234	4.74
Avg.	0.0182	1.207	0.181	0.424	0.464	0.659	0.149	2.48

All of the correlations, except that of Bons(18), used a roughness density parameter. The correlation of Sigal and Danberg(19) for three dimensional roughness, and the correlation of van Rij et al.(20) were about a third less than the correlations of Dvorak(21) and Dirling(22). The correlation of Waigh and Kind(23) and the two dimensional correlation of Sigal and Danberg showed greater equivalent height ratios than the other density based correlations. These density parameter correlations have much lower $h_{\mathrm{EQ}}/h_{\mathrm{RMS}}$ values than were obtained for the rough vane heat transfer tests discussed by Boyle et al.(24). The pitch-to-height ratios were greater in the present work.

The correlation used by Bons gives the roughness height as a function of the trace angle. Bons recommends that the angle be determined from the local trace angle. However, this was not done because the equivalent height ratio was sensitive to the spacing used for the digitized trace. Omitting every other point, reduced the $h_{\mathrm{EQ}}/h_{\mathrm{RMS}}$ by nearly thirty percent. In this table the angle was determined by the roughness height and pitch. For the widely spaced roughness assumption the peak increased less than the pitch, so that the roughness height was considerably less using Bons' correlation. When Bons' recommendation was used with all trace points, $h_{\mathrm{EQ}}/h_{\mathrm{RMS}}$ was very close to the values shown for $h_{\mathrm{PEAK}} > h_{\mathrm{AVG}}$.

For correlations based on a roughness density parameter, assuming cone shapes resulted in a somewhat higher equivalent roughness height, compared to hemispheres. The width of the cone base is determined from the roughness trace. The hemisphere assumption gives a base that is twice the height. The cone assumption, may be preferable, since it uses more information from the trace. The assumption of $h_{\mathrm{PEAK}} > h_{\mathrm{AVG}} + h_{\mathrm{RMS}}$, which results in widely spaced peaks, generally gives lower equivalent height ratios. The decrease is not consistent among the correlations. Since there are fewer peaks in each trace, a greater variation among the traces is not surprising. Koch and Smith(25) recommend that the equivalent height be taken as $6.2 \times h_{\mathrm{a}}$. Table III shows that this gives $h_{\mathrm{EQ}}/h_{\mathrm{RMS}} = 4.8$, or $h_{\mathrm{EQ}}/C = 8.4 \times 10^{-4}$.

It is generally accepted that surface roughness does not affect the boundary layer if the roughness height in wall units, $h^+ < 5$. An approximation for $h^+ < 5$ can be made using a flat plate analogy for adiabatic conditions.

$$h^+ = 0.17(h_{\mathrm{EQ}}/C)Re^{0.9}$$

When $h_{\mathrm{EQ}}/C = 8.4 \times 10^{-4}$, and $Re_{\mathrm{C}} = 1.1 \times 10^5$, $h^+ = 5$. The aft portion of the suction surface typically has an adverse pressure gradient with a decreased friction factor. Therefore, roughness effects are expected to be seen at Reynolds numbers greater than that given by the approximation. Values of $h_{\mathrm{EQ}}/C < 4.8 \times 10^{-4}$ give higher Reynolds numbers for the start of roughness effects.

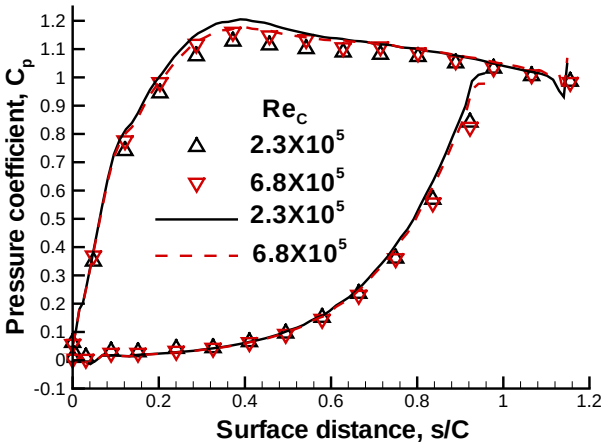

Fig. 3a Predicted and measured pressure coefficients, M_2=0.3

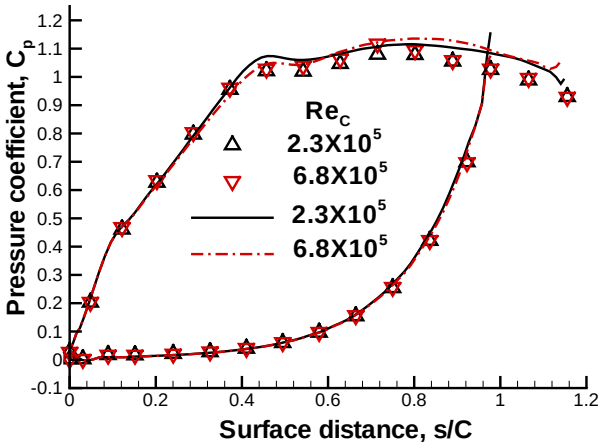

Fig. 3b Predicted and measured pressure coefficients, M_2=0.9

DESCRIPTION of ANALYSIS

Two dimensional analyses were done using the quasi-3D Navier-Stokes code RVCQ3D. This code has been documented by Chima (26), and by Chima and Yokota (27). C-type grids, typically 377 × 55, were used. Reference 24 gives a more detailed description of the analysis. The solutions were monitored to assure that convergence was achieved.

Loss predictions were obtained using both two-equation $k-\omega$ turbulence models, and using an algebraic model. These models were chosen because they gave reasonably accurate heat transfer predictions(24,28). Both low and high Reynolds number formulations of a $k-\omega$ turbulence model were compared with data. The algebraic turbulence model incorporated the Cebeci-Chang(11) roughness model. The implementation of these models in the analysis code is further discussed by Chima et al.(29) and Chima(30). In the algebraic turbulence model roughness serves to increase the mixing length. In the $k-\omega$ model roughness affects the wall boundary condition on ω

Algebraic turbulence model. The increase in the mixing length is given by:

$$\Delta y^+ = 0.9(\sqrt{h^+} - h^+ exp^{-0.167h^+})$$

and

$$\Delta y = \frac{\Delta y^+ \mu}{U_{\rm FS}\rho\sqrt{C_f/2}}$$

Only the inner region turbulent eddy viscosity, $\mu_{\rm t,i}$ is modified by roughness.

$$\mu_{\rm t,i} = \rho(dU/dy)\Big[\kappa(y+\Delta y)(1-exp^{-(y^+ + \Delta y^+)/A^+})\Big]^2$$

κ is the von Karman constant, and A^+ is a near wall damping coefficient.

Assuming fully turbulent flow over the entire surface will be shown to give larger than measured losses over much of the Reynolds number range. However, using a transition model suitable for smooth surfaces underpredicts losses at high Reynolds numbers. A transition criteria, incorporating surface roughness effects, is proposed, and is described when the experimental results are discussed.

$k-\omega$ turbulence model. In this model roughness influences the solution through the boundary condition on ω. At the vane surface $k=0$, and

$$\omega_0 = max\Big(\omega_{\rm IN}, max(2500/(h^+)^2, 100/h^+)dU/dy\Big)$$

and

$$\omega_{\rm IN} = \sqrt{1.5(U_{\rm IN}Tu_{\rm IN})^2}/l_{\rm IN}$$

Two implementations of the $k-\omega$ turbulence model are described by Chima(29). Results obtained using the high Reynolds number implementation are labeled H$k-\omega$. The low Reynolds number formulation results are labeled L$k-\omega$. The L$k-\omega$ formulation modifies the production and destruction terms by factors which are a function of the turbulent Reynolds number.

DISCUSSION of RESULTS

Surface pressures. Vane midspan surface pressures were only measured for the smooth vane. Figures 3a and 3b show pressure distributions for $M_2 = 0.3$, and 0.9. The lower Mach number C_p distribution is representative of forward loading, while the higher Mach number distribution represents aft loading. Neither the measured nor predicted C_p distributions show significant changes with Reynolds number variations. The pressure distributions show that the suction surface diffusion is relatively low. The adverse pressure gradient region is shorter at the higher Mach number. Predictions showed no variation between the smooth and rough surface pressure distributions.

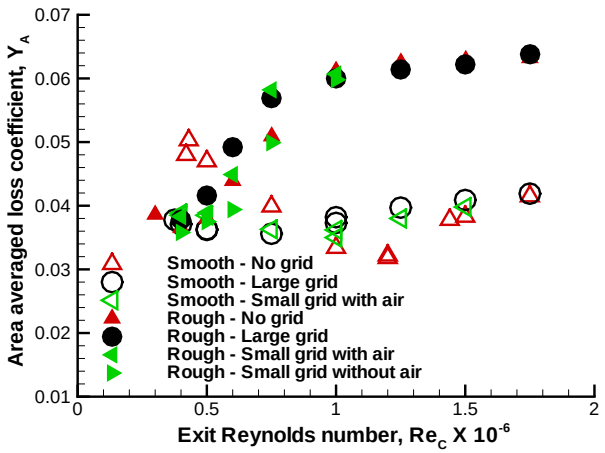

4a) Data for smooth and rough vanes

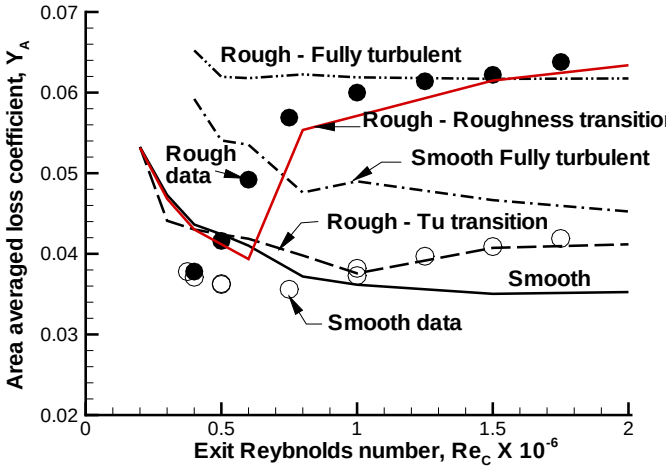

4b) Large grid - Cebeci-Chang roughness model

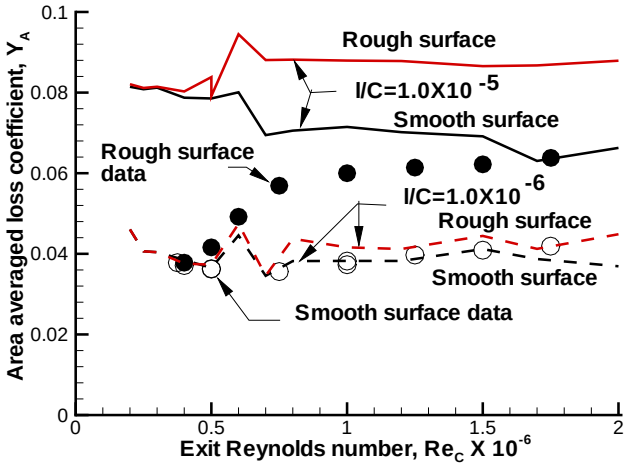

4c) Large grid data - Low Reynolds k-omega model

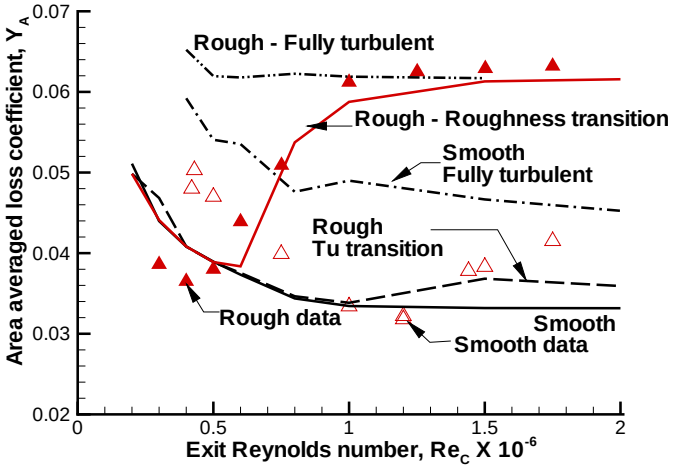

4d) No grid - Cebeci-Chang roughness model

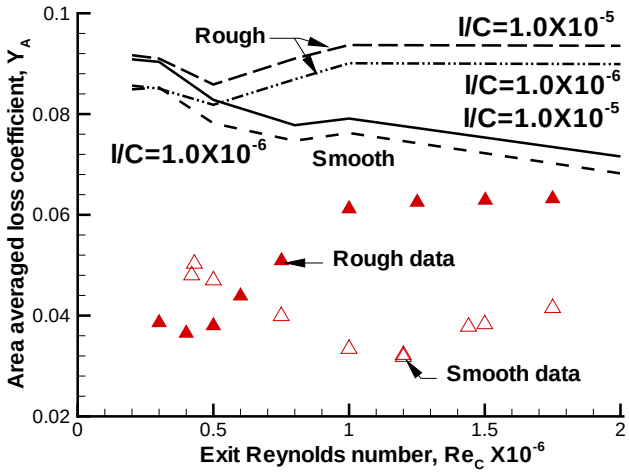

4e) No grid data Low Re k-omega model

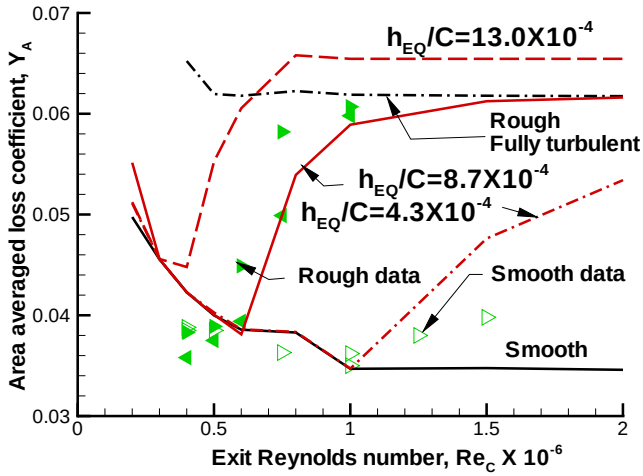

4f) Small grid data compared with Cebeci-Chang model

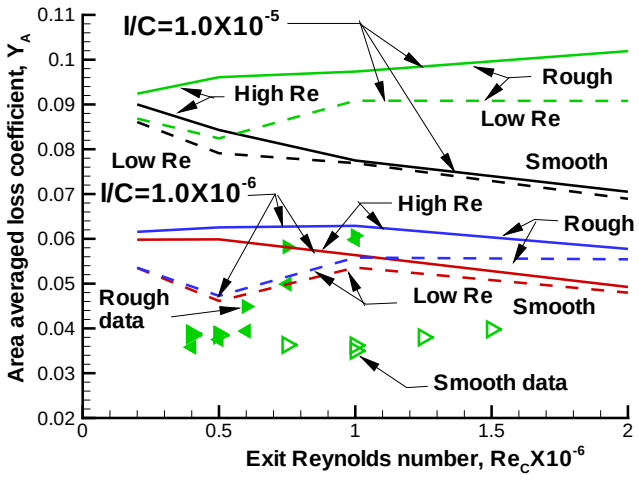

4g) Small grid data Low and High Re number k-omega model

Fig. 4 Predicted and measured loss at $M_2 = 0.9$.

Loss measurements. Figure 4 shows both smooth and rough vane average total pressure loss coefficients at the survey plane for a vane row exit Mach number of 0.9. Figure 4a shows just the experimental data. The smooth vane data are shown as open symbols, and the rough vane data as closed symbols. Different symbols denote different Tu levels. The different Tu levels are the result of using no grid, a large bar grid, and a small bar grid. The small bar grid has two symbols, to denote whether or not air was blown through the grid. Figures 4b through 4g show comparisons using different modeling assumptions.

Although the vane trailing edge is relatively thick, figure 4a shows that at high Reynolds numbers surface roughness nearly doubles vane loss at all three turbulence intensities. At high Reynolds numbers neither the smooth nor rough vane data show a sensitivity to turbulence intensity.

At low Reynolds numbers the smooth vane data show nearly a 40% loss increase for the no grid, low Tu, cases compared with the higher Tu cases. The rough vane data at low Tu shows no loss increase compared with the high Tu losses. The rough vane loss is not affected by turbulence intensity, and is as low as the smooth vane loss at high Tu. This beneficial effect of roughness at low Tu may result from roughness causing transition. This reduces the likelihood of separation. In contrast with the smooth vane data the rough vane data does not show the rapid rise in loss as Reynolds number is reduced. For these tests, the region over which roughness was beneficial was fairly small. These results are consistent with the observations of Pinson and Wang(31).

Figure 4a shows that as the Reynolds number is increased from 0.5×10^6 the rough vane shows a steady loss increase. After the Reynolds number has doubled, loss becomes independent of Reynolds number.

Figure 4b shows predictions using the Cebeci-Chang roughness model. Unless otherwise noted, a roughness to true chord, $h_{\rm EQ}/C$, of 8.4×10^{-4} was used, which corresponds to $h_{\rm EQ}/h_{\rm RMS} = 4.8$. Assuming that roughness causes fully turbulent flow, results in over predicting losses at low Reynolds numbers. Using just Mayle's(32) transition model causes only a gradual increase in loss. Even at $Re_C = 2 \times 10^6$ the predicted loss has not reached the asymptotic value.

A prediction is shown in figure 4b that attempts to account for the effects of roughness on transition. This prediction is labeled "Roughness transition". In this prediction the intermittency, τ is calculated from:

$$\tau = max(\tau_{\rm M}, \tau_{\rm R})$$

$\tau_{\rm M}$ is the intermittency calculated based on the flow parameters and local turbulence intensity. This value is calculated using Mayle's(32) transition start model, and the transition length model described by Boyle and Simon(33).

The roughness intermittency, $\tau_{\rm R}$, is based on the experimental data. The model uses the same form as models used to predict the start and length of transition from laminar to turbulent flow for smooth surfaces. The start of transition uses the form of Mayle's transition start model. In Mayle's model the start of transition is given by:

$$(Re_\theta)_{\rm START} = 400.0 Re_\theta Tu^{-0.625}$$

The roughness transition start model was similarly defined.

$$(Re_{\rm h})_{\rm START} = C_{\rm RS} Re_\theta (h_{\rm EQ}/\theta)$$

The intermittency for values of $Re_{\rm h} > (Re_{\rm h})_{\rm START}$ is:

$$\tau_{\rm R} = 1.0 - exp\Big(- C_{\rm RL}(Re_{\rm h} - (Re_{\rm h})_{\rm START})\Big)$$

$Re_{\rm h}$ is calculated from:

$$Re_{\rm h} = Re_\theta (h_{\rm EQ}/\theta)$$

The values of $C_{\rm RS}$ for the start of roughness transition, and of $C_{\rm RL}$ for the length of roughness transition, were determined to be 400 and 0.0077.

The suction and pressure surface roughnesses were equal, but the transition locations differed. The lower pressure surface inviscid velocities gave lower unit Reynolds number, Re_θ/θ, values.

Figure 4c shows comparisons using the L$k-\omega$ turbulence model. Predictions show an extreme sensitivity to inlet length scale, and poor agreement with rough vane data. The loss axis scale was expanded to accommodate the predictions. At $l/C = 1.0 \times 10^{-6}$ the analysis agrees very well with the smooth vane data. However, at this length scale no loss increase due to roughness is predicted, even at the highest Reynolds number. Increasing l/C to 1×10^{-5} gave very high predicted losses. The smooth vane prediction approaches twice the experimental loss levels. At this higher inlet length scale, the roughness loss increment is reasonably well predicted. However, the asymptotic loss exceeds measured values by more than two points.

Figure 4d compares predictions using the Cebeci-Chang roughness with data for the no grid, low turbulence intensity cases. Results are very similar to those for the large grid cases. The roughness transition model gives good agreement with the experimental rough vane data. The smooth vane prediction is lower than the smooth vane data except in the region near $Re_C = 1.0 \times 10^6$.

The low inlet turbulence intensity L$k-\omega$ results, shown in figure 4e, agree with neither the smooth nor rough vane data. In contrast with the results in figure 4c, the effects of inlet length scale are minor. The change in loss due to roughness is reasonably well predicted. However, the predicted loss levels are approximately twice those measured.

Figure 4f shows data for the small grid and predictions using Cebeci-Chang turbulence model. Predictions are also shown for variations of $\pm 50\%$ of the equivalent roughness, h_{EQ} A 50% change in equivalent height changes the asymptotic loss value approximately half a point. This indicates that the equivalent height ratio, h_{EQ}/h_{RMS}, for use in the analysis is close to 4.8 Where the predictions depart from the smooth prediction curve shows the sensitivity to C_{RS}, since $Re_h \propto C_{RS} h_{EQ}$. If a higher or lower roughness had a better asymptotic agreement, the constant C_{RS} and C_{RL} would have been changed.

Figure 4g compares L$k-\omega$ and H$k-\omega$ losses with the intermediate Tu - small grid data. The H$k-\omega$ losses are greater than the L$k-\omega$ model losses. But, even L$k-\omega$ results are much higher than the data.

$M_2 = 0.7$ results. The data in figure 5a for $M_2 = 0.7$ have many of the characteristics of the data in figure 4a for $M_2 = 0.9$. The minimum Reynolds number at $M_2 = 0.7$ is about 11% less than at $M_2 = 0.9$. For the no grid, low turbulence, cases the rough and smooth data show nearly the same loss levels at the minimum Reynolds number. The Reynolds number range over which roughness reduces loss is relatively narrow. In figure 5a this region is only from 3×10^5 to 5×10^5. There is close to a 2.5 point increase in loss due to roughness in the high Reynolds number region.

Predictions in figure 5b show the sensitivity of loss to the model used to predict the variation of turbulence intensity with freestream velocity. Reference 13 indicated that this variation was appropriately determined by the model of Steelant and Dick(34), and was used as the baseline model. An alternate approach assumes that the fluctuating velocity, u' remains constant throughout the passage. The choice of model affects smooth vane predictions. Figures 4 and 5 show that the baseline model underpredicts the experimental loss at high Reynolds numbers. Figure 5b shows that assuming u' constant gives a higher loss level. Most of the smooth vane data lie between these two predictions. The loss difference between the two models is most noticeable at high turbulence intensities. Although, not shown, predictions were found to be also sensitive to the artificial dissipation value. Higher values increased stability, but gave higher losses by up to half a point(0.005).

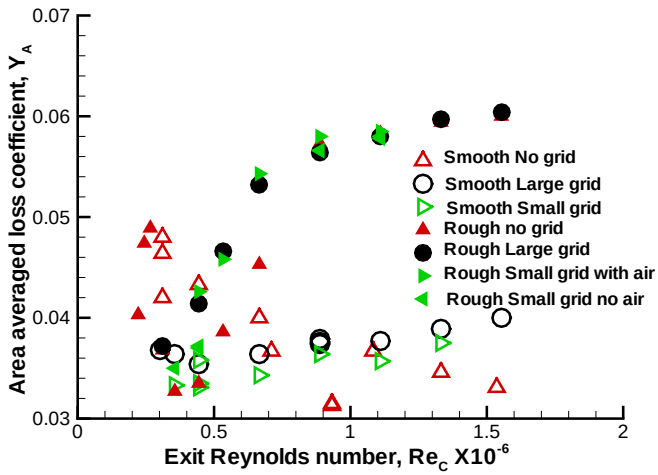

5a) Data for smooth and rough vane

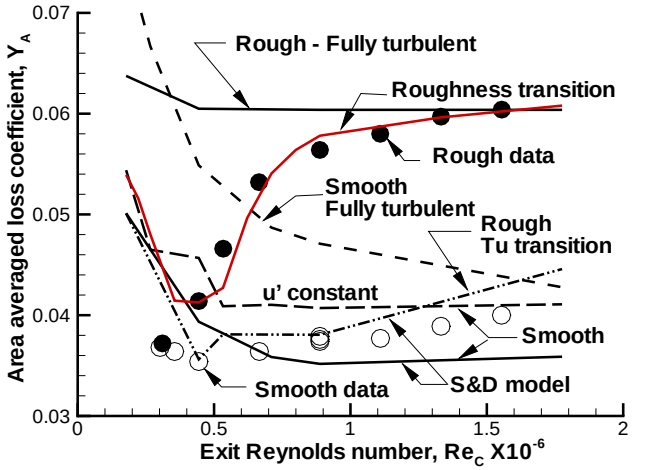

5b) Large grid - Cebeci-Chang roughness model

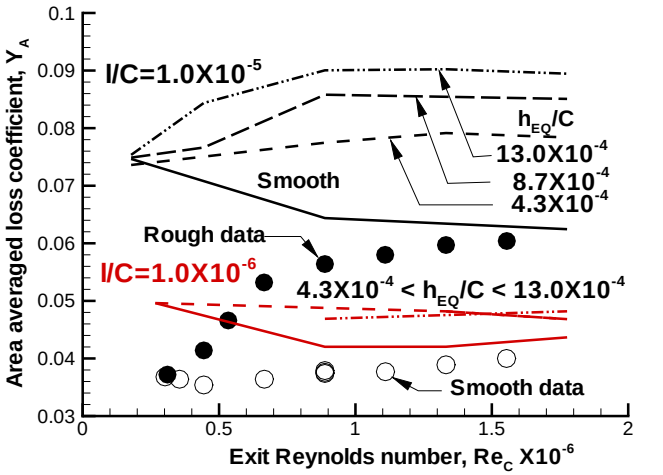

5c) Large grid data - Low Re k-omega model

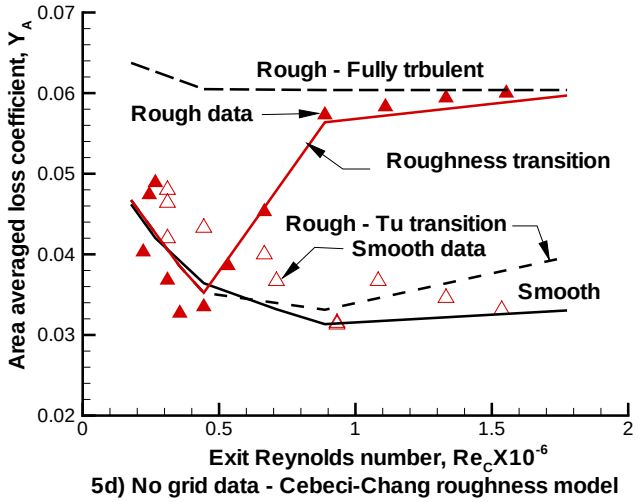

5d) No grid data - Cebeci-Chang roughness model

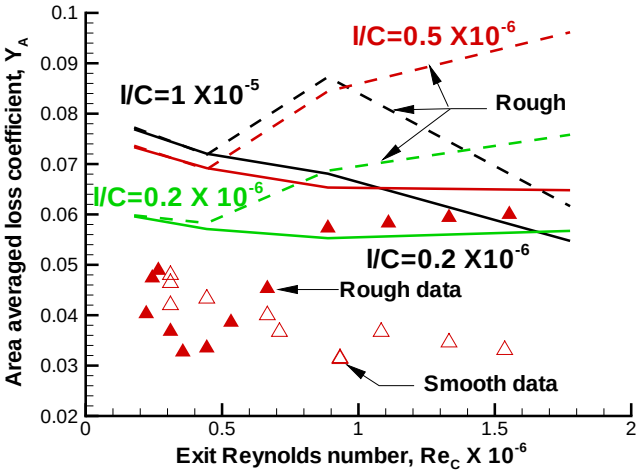

5e) No grid - Low Re k-omega model

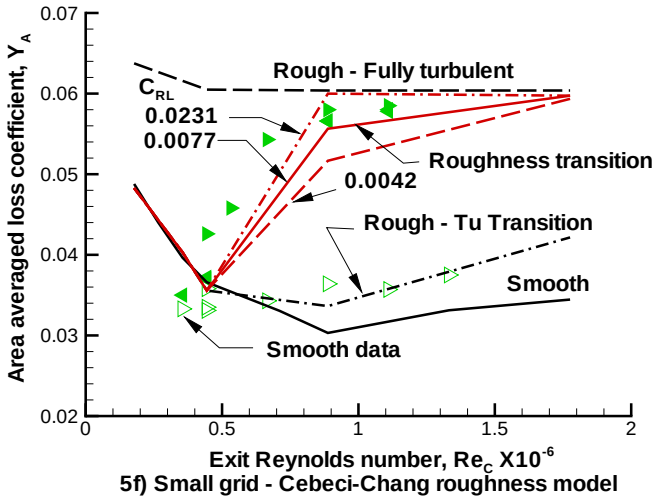

5f) Small grid - Cebeci-Chang roughness model

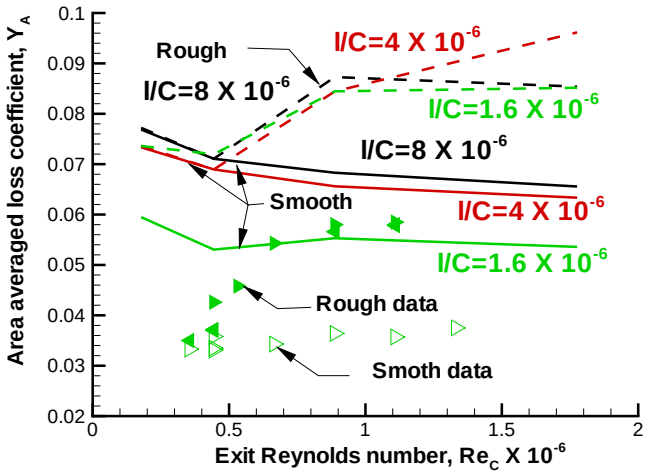

5g) Small grid Low Re k-omega model

Fig. 5 Predicted and measured loss at $M_2 = 0.7$.

Figure 5c shows comparisons with the large grid data using the L$k-\omega$ model. The results for the smaller inlet length scale show relatively good agreement with the smooth vane data at the higher Reynolds numbers. However, results for this length scale show only small loss increments due to roughness. For the range of roughness examined, the predicted loss level did not change with roughness. The results using the larger inlet length scale showed very high loss levels even for the smooth vane. At high Reynolds numbers the increase in loss with roughness is consistent with the data. Interestingly, the same roughness height, $h_{\mathrm{EQ}}/C = 8.4 \times 10^{-4}$, shows nearly the same increase in loss for either the Cebeci-Chang roughness model or the L$k-\omega$ model.

Figures 5d and 5f show comparisons with the no grid and small grid data. In both figures the roughness transition model agrees well with the rough vane data. Figure 5f shows the sensitivity of loss to different C_{RL} values. Lower value give shorter transition lengths, and a more rapid rise to the fully rough loss value.

Figures 5e and 5g show predictions using the L$k-\omega$ model at different inlet length scales. Similar to the results in figure 4, using constant values for the inlet length scale gives unsatisfactory agreement with the data. Menter(35) recommended that the freestream values for ω and the turbulent eddy viscosity, ν_{T}, be specified. The recommended values were $1 < \omega C/U < 10$ and $1.0 \times 10^{-5} < \nu_{\mathrm{T}}/\nu_{\mathrm{LAM}} < 1.0 \times 10^{-2}$. Since $k = \nu_{\mathrm{T}}\omega$, and k is known from measurements, inlet values for both ω and $\nu_{\mathrm{T}}/\nu_{\mathrm{LAM}}$ cannot be specified. Table V gives these two ratios as a function of Reynolds number, length scale, and turbulence intensity. The length scale used in the analysis is defined such that ω_{IN} is the same for both the H$k-\omega$ and L$k-\omega$ models. The inlet values for $\nu_{\mathrm{T}}/\nu_{\mathrm{LAM}}$ differ. Since $\omega C/U_{\mathrm{IN}}$ is much greater than the recommended value, specifying ω_{IN} is not useful.

Table V. Inlet characteristics.

			L $k-\omega$		H $k-\omega$
Tu	l/C	Re_C	$\omega C/U_{IN}$	ν_T/ν_{LAM}	ν_T/ν_{LAM}
17	1×10^{-5}	1.8×10^5	6.8×10^4	2.3×10^{-4}	8.6×10^{-3}
		8.9×10^5	6.8×10^4	1.4×10^{-3}	4.3×10^{-2}
		1.8×10^6	6.8×10^4	3.3×10^{-3}	8.6×10^{-2}
17	1×10^{-6}	1.8×10^5	6.8×10^3	3.3×10^{-3}	8.6×10^{-2}
		8.9×10^5	6.8×10^3	3.8×10^{-2}	4.3×10^{-1}
		1.8×10^6	6.8×10^3	1.3×10^{-1}	8.6×10^{-1}
8	1×10^{-5}	1.8×10^5	3.2×10^4	1.0×10^{-4}	4.0×10^{-3}
		8.9×10^5	3.2×10^4	5.7×10^{-4}	2.0×10^{-2}
		1.8×10^6	3.2×10^4	1.3×10^{-3}	4.0×10^{-2}
8	1×10^{-6}	1.8×10^5	3.2×10^3	1.3×10^{-3}	4.0×10^{-2}
		8.9×10^5	3.2×10^3	1.1×10^{-2}	2.0×10^{-1}
		1.8×10^6	3.2×10^3	3.5×10^{-2}	4.0×10^{-1}
1	1×10^{-5}	1.8×10^5	4.0×10^3	1.3×10^{-5}	5.0×10^{-4}
		8.9×10^5	4.0×10^3	6.4×10^{-5}	2.5×10^{-3}
		1.8×10^6	4.0×10^3	1.3×10^{-5}	5.0×10^{-3}
1	1×10^{-6}	1.8×10^5	4.0×10^2	1.3×10^{-4}	5.0×10^{-3}
		8.9×10^5	4.0×10^2	7.3×10^{-4}	2.5×10^{-2}
		1.8×10^6	4.0×10^2	1.7×10^{-3}	5.0×10^{-2}

Calculations were done where the inlet value of ν_T/ν_{LAM} was specified. The agreement with the experimental data was not improved using this approach.

The difficulties associated with the $k-\omega$ model suggest that utilizing the SST model proposed by Menter(35) might be beneficial. This model was proposed to reduce the sensitivity of the results to the freestream values of ω.

Table V shows that ν_T/ν_{LAM} is much larger for the H$k-\omega$ model, than for the L$k-\omega$ model, and that ω_{IN} can be very large. ω_{IN} was used as a lower bound on ω_0, to prevent ω_0 from going to zero. Since ω_0 is likely to be higher for a smooth surface than for a rough one, using ω_{IN} to set the wall boundary condition appears to be inappropriate. Limiting either k or ω should be evaluated when predicting rough surface behavior.

$M_2 = 0.5$ results. Figure 6a compares experimental loss data for $M_2 = 0.5$. Results are similar to those at the higher Mach numbers. The rough vane losses for the cases of the small grid with air exceeded the large grid losses. But, without air the small grid losses were close to the large grid and no grid losses. At high Reynolds numbers, roughness causes a loss increase of 2.5 points. Figures 6b-d show that the roughness transition model correctly predicts the increase in loss with Reynolds number. Only for the large grid with high turbulence intensity does the longer transition length give better agreement with data. Figure 6b also shows the effect of different variations of turbulence intensity with freestream velocity. Except at the highest Reynolds number, the Steelant and Dick model gives the better data agreement.

$M_2 = 0.3$ results. Figure 7 shows results for $M_2 = 0.3$. At this low Mach number there was greater scatter in the loss coefficient, Y_A, due to small unavoidable variations in the inlet total pressure during a survey. Still, the experimental data are consistent with those at higher Mach

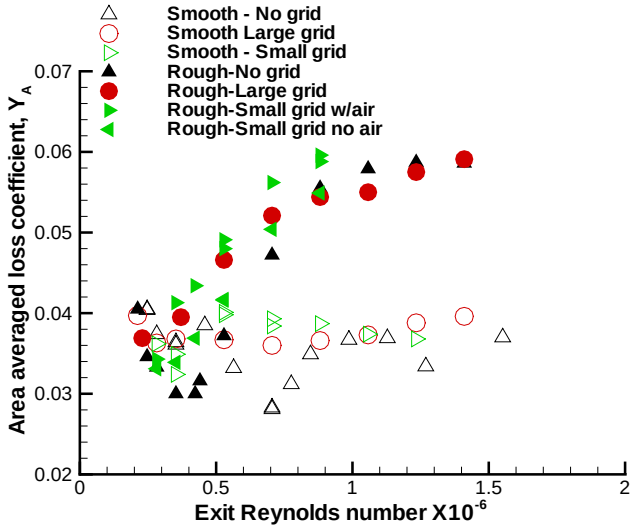

6a) Comparison of smooth and rough vane loss

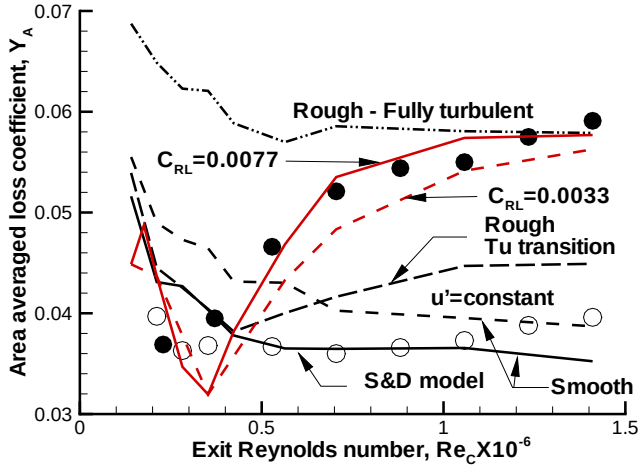

6b) Large grid data - Cebeci Chang roughness model

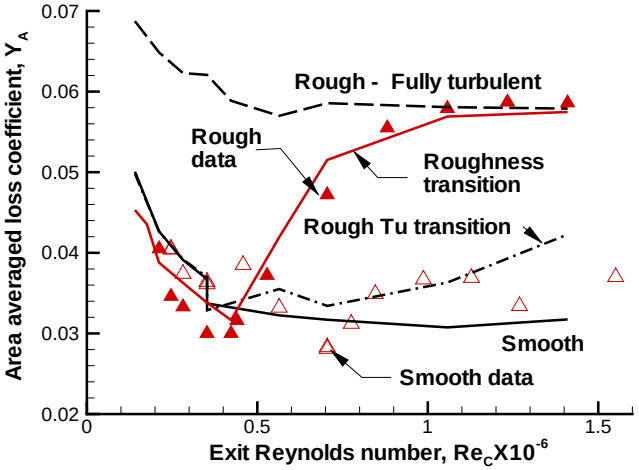

6c) No grid - Cebeci Chang roughness model

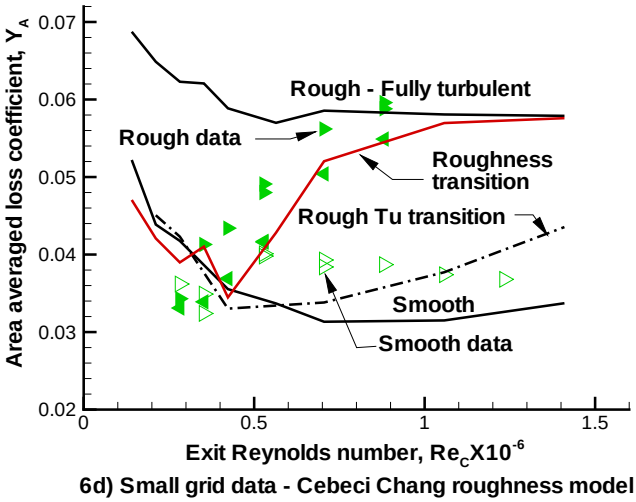

6d) Small grid data - Cebeci Chang roughness model

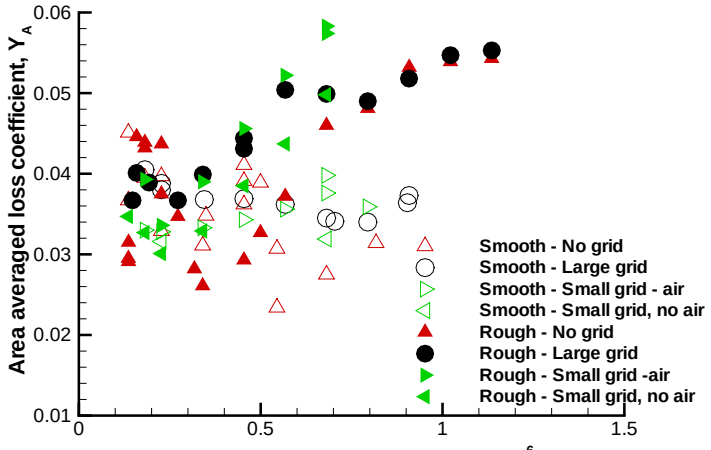

7a) Comparison of smooth and rough vane loss data

Fig. 6 Predicted and measured loss at $M_2 = 0.5$.

numbers. The analyses predict the data about as well as they did at the higher Mach numbers. For $M_2 = 0.3$ a longer transition length is appropriate. Figure 3 shows that the suction surface adverse pressure gradient is largest at $M_2 = 0.3$. While normal transition generally occurs faster in an adverse pressure gradient, the momentum thickness is also rapidly growing. The longer transition length may be the result of h^+/θ being lower in adverse pressure gradients.

Figure 7d shows the effects of varying the transition start location, while holding C_{RL} constant. The curves are approximately parallel in the transition region. Using a transition length that is proportional to the Reynolds number at transition start, affects the curve shape less than varying C_{RL}.

CONCLUSIONS

Vane surface roughness effects on loss strongly depend on Reynolds number. At fairly low Reynolds numbers, corresponding to low h^+ values, roughness reduced loss at low turbulence intensities, and did not increase loss at higher turbulence intensities. Small h^+ values promote transition, and lowers losses that are probably due to laminar separation. This occurred over only a small Reynolds number range. At the lowest Reynolds numbers the smooth and rough vane losses were the same, and relatively high. At high Reynolds numbers, roughness nearly doubled the loss levels. Transition from low to high losses occurred as the Reynolds number doubled.

The best data agreement was achieved using the Cebeci-Chang roughness model in conjunction with a roughness transition model. This approach, which can be used in Navier-Stokes and boundary layer analyses, can be used for for loss prediction for non-uniformly distributed roughness. To analyze roughness effects, the roughness

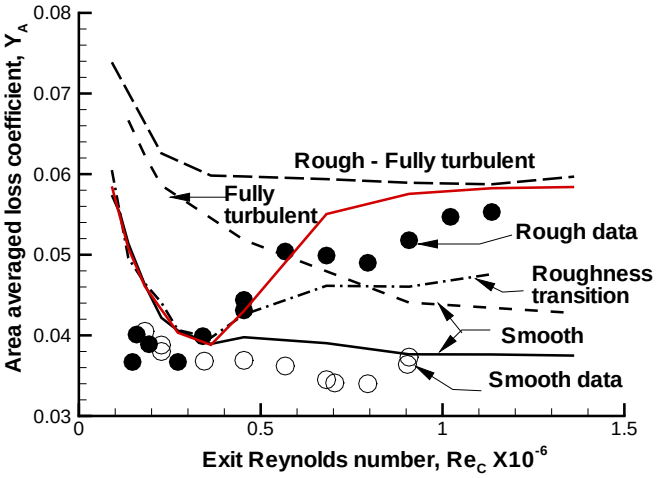

7b) Large grid data - Cebeci Chang roughness model

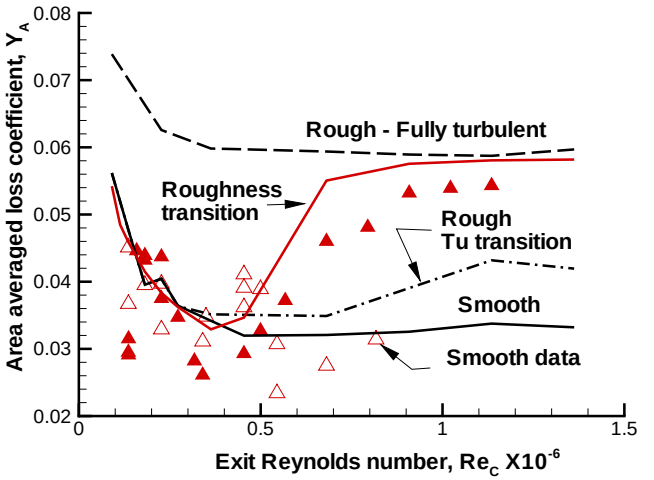

7c) No grid data - Cebeci Chang roughness model

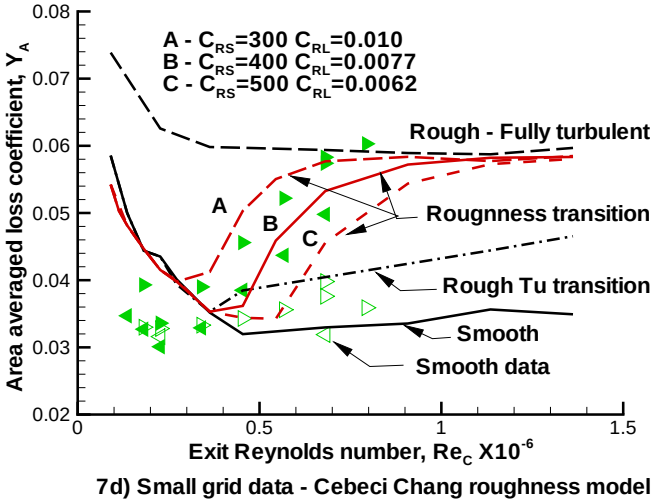

Fig. 7 Predicted and measured loss at $M_2 = 0.3$.

height would be given as a function of surface distance. The Cebeci-Chang roughness model is implemented in an algebraic turbulence model. Without a roughness transition model, losses were underpredicted because the model accounted for roughness only after transition began. Assuming turbulent flow from the leading edge resulted in high loss levels. Only at very high Reynolds numbers did the predicted losses for fully turbulent flow approach the measured losses.

$k-\omega$ turbulence model predictions were not satisfactory. Predicted losses were highly sensitive to $\omega_{\rm IN}$, which was determined from the inlet length scale. No satisfactory means of specifying this length scale was found. Lowering the length scale increases $\omega_{\rm IN}$. Predictions with high $\omega_{\rm IN}$ values agreed reasonably well with the smooth vane loss data, but only gave small loss increases due to roughness. Lower values gave predictions which showed loss increases due to roughness that approximated those seen in the data. However, these lower values had smooth vane losses far greater than the data. The $k-\omega$ results were generally less sensitive to Reynolds number than either the data or the algebraic model results. The difficulties associated with the model may be due to transition like effects. Often the $k-\omega$ model gave losses close to those obtained by assuming fully turbulent flow.

The same value for $h_{\rm EQ}/C = 8.4 \times 10^{-4}$ resulted in good agreement between predictions and data for almost all test conditions. This corresponds to an average $h_{\rm EQ}/h_{\rm RMS}$ value of 4.8, and a $h_{\rm EQ}/h_{\rm a}$ value of 6.2. This agrees very well with the recommended value from Koch and Smith(25). The approach recommended by Bons(18) also gives ratios in this range. However, the equivalent height is strongly dependent on the angle used for the roughness. The $h_{\rm EQ}/C$ ratios calculated from roughness density parameters were close to one or less. The roughness density approach resulted in equivalent height ratios consistent with predictions for roughness effects on turbine blade heat transfer,(Boyle et al.(24)). However, here this approach gave low equivalent height ratios, which would underpredict the effects of roughness on loss. The roughness characteristics in that experiment were much different from the roughness of the vanes tested in this experiment. The skewness and kurtosis were both close to -0.5, whereas here the skewness was close to zero, and the kurtosis less than -1.0. Van Rij et al.(20) recommend that a three dimensional roughness trace be used to determine the equivalent roughness height. The low values in Table IV for the equivalent height, obtained by using just the two dimensional trace, support this recommendation.

Predicted smooth vane losses were sensitive to the assumption regarding how the velocity fluctuations varied with the inviscid velocity. Using the model of Steelant and Dick(33) often improved agreement with data. The smooth vane data typically showed a minimum loss near $Re_{\rm C} = 750,000$. The Steelant and Dick model resulted in good agreement with data in this region. However, at the highest Reynolds numbers, this model predicted lower than measured losses. In this region assuming that the velocity fluctuations remained constant gave better agreement with data.

Predicted losses were affected by the value of artificial dissipation, and this effect was more noticeable for the smooth vane. The same grid was used for all calculations. A higher value of artificial dissipation was sometimes needed at low Reynolds numbers. This could be one of the contributing factors as to why the analysis tended to overpredict losses at low Reynolds numbers.

Acknowledgement
We would like to acknowledge the help of Kevin Radil for the surface roughness measurements.

REFERENCES

(1) Kind, R.J., Serjak, P.J., and Abbott, M.W.P., 1998, "Measurements and Prediction of the Effects of Surface Roughness on Profile Losses and Deviation in a Turbine Cascade," ASME *Journal of Turbomachinery,* Vol. 120, pp. 20-27.

(2) Boynton, J.L., Tabibzadeh, R., and Hudson, S.T., 1992, "Investigation of Rotor Blade Roughness Effects on Turbine Performance," ASME *Journal of Turbomachinery,* Vol. 115, pp. 614-620.

(3) Bammert, K., and Stanstede, H., 1972, "Measurements Concerning the Influence of Surface Roughness and Profile Changes on the Performance of Gas Turbines," ASME *Journal of Engineering for Power,* Vol. 94, pp. 207-213.

(4) Bammert, K., and Stanstede, H., 1976, "Influences of Manufacturing Tolerances and Surface Roughness of Blades on the Performance of Turbines," ASME *Journal of Engineering for Power,* Vol. 98, pp. 29-36.

(5) Harbecke, U.G., Riess, W. and Seume, J.R., 2002, "The Effect of Milling Process Induced Coarse Surface Texture on Aerodynamic Turbine Profile Losses," ASME paper GT-2002-3033

(6) Stabe, R.G., and Liebert, C.H., 1975, "Aerodynamic Performance of a Ceramic-Coated Core Turbine Vane Tested with Cold Air in a Two-Dimensional Cascade", NASA TM X=3191.

(7) Bons, J.P., Taylor, R.P., McClain, S.T., and River, R.B., 2001, "The Many Faces of Turbine Surface Roughness, ASME *Journal of Turbomachinery,* Vol. 123, pp. 739-748.

(8) Taylor, R.P., 1990, "Surface Roughness Measurements on Gas Turbine Blades," ASME *Journal of Turbomachinery,* Vol. 112, pp. 175-180.

(9) El-Batsh, H., and Haselbacher, H., 2002, "Numerical Investigation of the Effects of Ash Particle Deposition on the Flow Field Through Turbine Cascades," ASME paper GT-2002-30600

(10) Taylor, R.P, Coleman, H.W., and Hodge, B.k., 1985, "Predictions of Turbulent Rough-Wall Skin Friction Using a Discete Element Approach," ASME *Journal of Fliuds Engineering,* Vol. 107, pp. 251-257.

(11) Cebeci, T., and Chang, K.C., 1978, "Calculation of Incompressible Rough-Wall Boundary Layer Flows," AIAA *Journal,* Vol. 16, No. 7, pp 730-735.

(12) Wilcox, D.C., 1994, *Turbulence Modeling for CFD,* DCW Industries, Inc, La Canada, CA.

(13) Boyle, R.J., Lucci, B.L, and Senyitko, R.G., 2002, "Aerodynamic Performance and Turbulence Measurements in a Turbine Vane Cascade", ASME paper GT-2002-30434

(14) Boyle, R.J., Lucci, B.L., Verhoff, V.G., Camperchioli, W.P., and La, H., 1998, "Aerodynamics of a Transitioning Turbine Stator Over a Range of Reynolds Numbers," ASME paper 98-GT-285.

(15) Price, J., Jimenez, O., Miriyala, N., Kimmel, J.B., Leroux, D.R., and Fahme, T., 2001, "Ceramic Stationary Gas Turbine Development Program - Eighth Annual Summary," ASME paper 2001-GT-0517.

(16) Schwab, J.R., 1982, "Aerodynamic Performance of High Turning Core Turbine Vanes in a Two-Dimensional Cascade," NASA TM 82894.

(17) Abuaf, N., Bunker, R.S., and Lee, C.P., 1998, "Effects of Surface Roughness on Heat Transfer and Aerodynamic Performance of Turbine Airfoils," ASME *Journal of Turbomachinery,* Vol. 120, pp. 522-529.

(18) Bons, J.P., 2002, "St and C_f Augmentation for Real Turbine Roughness with Elevated Freestream Turbulence," ASME paper GT-2002-30198.

(19) Sigal, A., and Danberg, J.E., 1990, "New Correlation of Roughness Density Effect on the Turbulent Boundary Layer," AIAA *Journal,* Vol. 28, No. 3, pp 554-556.

(20) van Rij, J.A., Belnap, B.J., and Ligrani, P.M., 2002, "Analysis and Experiments on Three-Dimensional, Irregular Surface Roughness," ASME *Journal of Fluids Engineering,* Vol. 124, pp. 671-677.

(21) Dvorak, F.A., 1969, "Calculation of Turbulent Boundary Layers on Rough Surfaces in Pressure Gradient," AIAA *Journal,* Vol. 7, No. 9, pp 1752-1759.

(22) Dirling, R.B., 1973, "A Method for Computing Roughwall Heat Transfer Rates on Re-Entry Nosetips," AIAA paper 73-763

(23) Waigh, D.R., and Kind, R.J., 1998, "Improved Aerodynamic Characterization of Regular Three-Dimensional Roughness," AIAA *Journal,* Vol. 36, No. 6, pp 1117-1119.

(24) Boyle, R.J., Spuckler, C.M. and Lucci, B.L., 2000, "Comparison of Predicted and Measured Turbine Vane Rough Surface Heat Transfer," ASME paper 2000-GT-0217

(25) Koch, C.C., and Smith, L.H., 1976, "Loss Sources and Magnitudes in Axial-Flow Compressors," ASME *Journal of Engineering for Power,* Vol. 98, pp. 411-424.

(26) Chima, R.V., 1987 "Explicit Multigrid Algorithm for Quasi-Three- Dimensional Flows in Turbomachinery." AIAA *Journal of Propulsion and Power,* Vol. 3, No. 5, pp. 397-405.

(27) Chima, R.V., and Yokota, J.W., 1990, "Numerical Analysis of Three-Dimensional Viscous Internal Flows," AIAA *Journal,* Vol. 28, No. 5, pp. 798-806.

(28) Ameri, A.A., and Bunker, R.S., 1999, "Heat Transfer and Flow on the First Stage Blade Tip of a Power Generation Gas Turbine; Part 2: Simulation Results," ASME paper 99-GT-283, (NASA CR-1999-209151).

(29) Chima, R.V., Giel, P.W., and Boyle, R.J., 1993 "An Algebraic Turbulence Model for Three-Dimensional Viscous Flows," AIAA paper 93-0083, (NASA TM-105931).

(30) Chima, R.V., 1996, "Application of the $k-\omega$ Turbulence Model to Quasi-Three-Dimensional Turbomachinery Flows," AIAA *Journal of Propulsion and Power,* Vol. 12, No. 6, pp. 1176-1179.

(31) Pinson, M.W., and Wang, T., 2000 "Effect of Two-Scale Roughness on Boundary Layer Transition over a Heated Flat Plate: Part 1 - Surface Heat Transfer,"ASME *Journal of Turbomachinery,* Vol. 122, pp. 301–307.

(32) Mayle, R.E., 1991, "The Role of Laminar-Turbulent Transition in Gas Turbine Engines", ASME *Journal of Turbomachinery,* Vol. 113, pp. 509-537.

(33) Boyle, R.J, and Simon, F.F., 1999, "Mach Number Effects on Turbine Blade Transition Length Prediction," ASME *Journal of Turbomachinery,* Vol. 121, pp. 694-702.

(34) Steelant, J. and Dick, E., 1999 "Prediction of By-Pass Transition By Means of a Turbulence Weighting Factor - Part I: Theory and Validation," ASME paper 99-GT-29.

(35) Menter, F., 1994, "Influence of Freestream Values on $k-\omega$ Turbulence Model Predictions," AIAA *Journal,* Vol. 32, No. 8, pp. 1598-1605.